


Antitumor and Antibacterial Efficacy of Gallium Nanoparticles Coated by Ellagic Acid

Sawsan M El-sonbaty¹, Fatma SM Moawed² , Eman I Kandil³  and Amira M Tamamm³

Dose-Response:
An International Journal
January-March 2022: 1–15
© The Author(s) 2022
Article reuse guidelines:
sagepub.com/journals-permissions
DOI: 10.1177/115593258211068998
journals.sagepub.com/home/dos


Abstract

Cancer is a mortality contributor worldwide, and breast cancer is the most common among women. Despite the numerous breast cancer therapeutic strategies, they either have limitations or sometimes are resisted by cancer, so new approaches are needed to tackle those restrictions. Nanotechnology offers exciting leaps in the diagnosis and treatment of cancer, especially breast cancer. The main objective of this study was to investigate the effect of the newly synthesized gallium nanoparticles coated by Ellagic acid (EA-GaNPs) on the induced mammary gland carcinogenesis in female rats and their antibacterial activities comparison with standard antibiotics (Ketoconazole (100 µg/ml) and Gentamycin (4 µg/ml)) by disc diffusion method using eight different microbial species. The antitumor efficacy of EA-GaNPs was conducted both *in vitro* and *in vivo*. The result of antimicrobial activity of EA-Ga NPs (1 mg/1 mL) revealed moderate toxicity behavior against Gram-positive (*Staphylococcus aureus*, *Bacillus subtilis*, *Bacillus cereus*) and Gram-negative pathogenic bacteria (*Escherichia coli*, *Proteus vulgaris*) also, antifungal activity was detected against (*Aspergillus terreus*). *In vitro* study showed that EA-GaNPs inhibited human breast cancer cell line (MCF-7) proliferation with IC₅₀ of 2.86 µg/ml. Although *in vivo*; the administration of EA-GaNPs to DMBA-treated rats ameliorated the hyperplastic state of mammary gland carcinogenesis induced by DMBA. Additionally, EA-GaNPs administration significantly modulated the activities of ALT and AST, as well as the levels of urea and creatinine in serum. Also, EA-GaNPs administration improved the antioxidant state by increasing Superoxide dismutase activity and GSH content, and decreasing malondialdehyde content in the mammary tissue, besides enhancing the apoptotic activity through elevating the levels of caspase-3 and decreasing the protein intensities of protein kinase B & phosphatidyl inositide 3-kinases. Furthermore, a significant decrease in serum Total iron-binding capacity accompanied by a significant increase in the level of calcium was noted. So, it can be concluded that the newly synthesized nanoparticles EA-GaNPs have an efficient antitumor activity that was manifested by reduction of the viability on the human breast cancer cell line (MCF-7) *in vitro*. Also, *in vivo* against the chemically induced mammary gland carcinogenesis in a female rat model. Histopathological findings were in harmony with biochemical and molecular results showing the effectiveness of EA-GaNPs against mammary carcinogenesis. Therefore, EA-GaNPs could be a promising, potent anti-cancer compound.

Keywords

EA-GaNPs, 7, 12-Dimethylbenz[a] Anthracene, protein kinase B, phosphatidyl inositide 3-kinases, Caspase-3, antioxidants

Introduction

Breast cancer is the most frequently diagnosed cancer among women worldwide accounting for almost 1 in 4 female cancer cases and is considered as the second leading cause of cancer death with nearly 2.1 million new cases diagnosed in 2018, accounting for 11.6% of all newly diagnosed cancer cases and 6,6 % of all Cancer Deaths in 2018.¹

Increasing incidence and mortality of breast cancer ascribed to various risk factors, the predominant LSD factors are genetic vulnerability (mutations in BRCA 1 and BRCA 2), exposure to radiation, overweight and obesity, and alcohol addiction. Furthermore, breast cancer is associated with age

¹Radiation Microbiology Department, National Center for Radiation Research and Technology, Egyptian Atomic Energy Authority, Cairo, Egypt

²Health Radiation Research Department, National Center for Radiation Research and Technology, Egyptian Atomic Energy Authority, Cairo, Egypt

³Biochemistry Department, Faculty of Science, Ain Shams University, Cairo, Egypt

Received 30 December 2021; accepted 6 December 2021

Corresponding Author:

Eman I Kandil, Biochemistry Department, Faculty of Science, Ain Shams University, Abbassia, Cairo 00202, Egypt.
Email: kandil.eman@yahoo.com



Creative Commons Non Commercial CC BY-NC: This article is distributed under the terms of the Creative Commons Attribution-NonCommercial 4.0 License (<https://creativecommons.org/licenses/by-nc/4.0/>) which permits non-commercial use, reproduction and distribution of the work without further permission provided the original work is attributed as specified on the SAGE

and Open Access pages (<https://us.sagepub.com/en-us/nam/open-access-at-sage>).

and estrogen exposure. Steroidal hormone, principally estrogen, can cause the induction and growth of breast cancer.²

Breast cancer is usually treated with surgery, which may be followed by chemotherapy or radiation therapy, or both. Those conventional breast cancer therapies have limitations as they are not usually successful in curing metastatic stages.³ Also, radio or chemotherapeutic agents are not targeted sufficiently; cause systemic effects and have poor penetration at the intended treatment site.⁴

Pathogenic microbes are considered a serious problem as cancer may be stimulated by microbial infection and remain a serious problem in patients with advanced cancer. Thus, most patients treated with antineoplastic drugs are potential recipients of antimicrobial drugs. Very often these drugs have to be given in combination. Although synergistic and antagonistic actions between antibacterial drugs have been well documented, that raised the need for anticancer drugs to have the activity against bacterial infections, which enhanced researchers for repurposing of anticancer drugs for the treatment of bacterial infections.⁵

Therefore, there is a need for new strategies or a new generation of drugs that can overcome those limitations. Nanotechnology, through using nanoparticles, offers exciting leaps forward in the diagnosis and treatment of cancer which tackles the limitations of conventional therapeutic strategies. The therapeutic approaches of nanoparticles are based on rectifying the damaging mechanism of the genes or by stopping the blood supply to the cancer cells or destroying the cancer cells themselves.⁶ Due to the advantages of nanoparticles as they have a high surface area to volume ratio which allows many functional groups to be attached to a nanoparticle, which also can seek out and bind to certain tumor cells.⁷

Additionally, the small size of nanoparticles (1 to 100 nm), allows them to accumulate at tumor sites.⁸ Recently and because of the medical importance of nanoparticles, they have been synthesized biologically via eco-friendly, cost-effective methods using microorganisms, enzymes, fungus and plants or plant extracts.⁹

Gallium (Ga) is considered the second metal after platinum with clinical antitumor activity.¹⁰ The antiproliferative activity of Ga depends mainly on the mimic action of Ga³⁺ with Fe³⁺, so Ga acts on cellular iron-dependent processes at various points in the cell to disrupt tumor growth.¹¹

Ellagic acid (EA) naturally occurring polyphenolic constituent that is contained in many fruits and nuts as grapes, pomegranate, red raspberry, strawberry, blueberry, walnuts, and cashew nuts,¹² is known for its potent antioxidant activity, radical scavenging capacity, chemopreventive and anti-apoptotic properties.¹³ *In vitro* and *in vivo* experiments have revealed that EA elicits anticarcinogenic effects by inhibiting tumor cell proliferation, inducing apoptosis, breaking DNA binding to carcinogens, blocking virus infection, and disturbing inflammation, angiogenesis, and drug-resistance processes required for tumor growth and metastasis.¹²

Accordingly, the main object of this study was to investigate the effect of the newly synthesized gallium nanoparticles coated

by Ellagic acid (EA-GaNPs) on the induced mammary gland carcinogenesis in female rats.

Due to the fact of relying on the basic mechanism of cancer development primarily on DNA damage-induced through several protein clusters and pathways (signaling pathways), the present work studied the antitumor effect of the newly synthesized nanoparticles through proteomic quantitation of two selected candidate proteins (phosphatidylinositol 3-kinases (PI3K) and protein kinase B (AKT)) by western blot, as the PI3K-AKT-mTOR pathway is one of the most frequently deregulated pathways in cancer as it controls key cellular processes, such as metabolism, motility, growth, and proliferation, that support the survival, expansion and dissemination of cancer cells, in addition to the oncogenic activation of the PI3K-AKT-mTOR pathway often occurs alongside pro-tumorigenic aberrations in other signaling networks.¹⁴ Also, the antimicrobial activity of the newly synthesized gallium nanoparticles coated by Ellagic acid (EA-GaNPs) was also evaluated in comparison with standard antibiotics (Ketoconazole (100 µg/ml) and Gentamycin (4 µg/ml)) by disc diffusion method using eight different microbial species.

Methods

Chemicals

7, 12-Dimethylbenz[a] Anthracene (DMBA) Was Purchased from Sigma-Aldrich Company, Saint Louis, Missouri, USA. Gallium Nitrate and Ellagic Acid Were Purchased from Sigma-Aldrich Company, Saint Louis, Missouri USA.

Cell Line

Human breast cancer (MCF-7) cell line was obtained from VACSERA Tissue Culture Unit.

Experimental Animals

Female Swiss albino rats (50-60 days old) weighing (120 ± 20 gm.) were obtained from the breeding unit of the National Research Centre (NRC), Cairo, Egypt. They were used for the *in vivo* study to determine the median lethal dose (LD50) and antitumor efficacy of the EA-GaNPs. The animals were housed in the animal house of the National Center for Radiation Research and Technology (NCRRT), Cairo, Egypt under standard laboratory conditions. Animals were maintained on a high protein commercial diet and water *ad libitum* and they were maintained for one week before starting the experiment as an acclimatization period.

Ethics Statement

The study was conducted by international guidelines for animal experiments and approved by the Ethical Committee at the National Center for Radiation Research and Technology (NCRRT), Atomic Energy Authority, Cairo, Egypt.

Chemical Study

Synthesis and Characterization of EA-GaNPs:

Gallium nanoparticles coated by Ellagic acid were synthesized (EA-GaNPs) referring to the method in the literature of Li,¹⁵ First, 2 mL of (Ga (NO₃)₃) (20 mM) was added to 46 mL of double-distilled water under magnetic stirring at room temperature. Then 2 mL of EA (10 mM) was added, and the pH value was adjusted to 11.0 with 1.0 M NaOH. Then the reaction was maintained at room temperature for 30 min. The nanoparticles were condensed and purified by centrifugation at 15 000 r.p.m for 10 min. and washed with double-distilled water three times.

Characterization of the EA-GaNPs:

Dynamic light scattering (DLS):

Sample of EA-GaNPs was analyzed for size dimensions by (DLS Zetasizer Nano ZS ZEN 3600, Malvern, UK).

Ultraviolet-visible absorption (UV/VIS) Spectroscopy:

The ultraviolet-visible spectrum of EA-GaNPs was analyzed using (the computerized double-beam ultraviolet-visible Jenway 6505 spectrophotometer, Keison, UK). The ultraviolet spectrum for EA-GaNPs sample was obtained by exposing the sample to visible light at a range of 200–900 nm. Deionized water was used for background correction of all ultraviolet-visible spectra.

Scanning electron microscope (SEM) Analysis:

A scanning electron microscope (SEM) was used to identify the size, shape and morphology of EA-GaNPs using (JEOL, JSM-5400 Scanning Microscope, FEJ EUROPE, Benelux). The sample was prepared and allowed to evaporate before analysis using JEOL, JFC-1100E Ion Sputtering Device.

Fourier transforms infrared spectroscopy (FT-IR):

Samples of EA-GaNPs and EA used for the nanoparticle synthesis were analyzed for the functional group using (VERTEX 70 FT-IR Spectrometer, BRUKER) scanned in the range of 4000–400 cm⁻¹.

Antimicrobial Assay of EA-GaNPs

The antibacterial activities of biosynthesized EA-GaNPs and standard antibiotics, including Ketoconazole (100 µg/mL), Gentamycin (4 µg/mL), were evaluated by disc diffusion method by using eight different microbial species: *Aspergillus flavus*, *Candida albicans*, *Aspergillus terreus*, *Staphylococcus aureus*, *Bacillus subtilis*, *Bacillus cereus*, *Escherichia coli*, and *Proteus vulgaris*. Fungi strains were cultured on Sabouraud Dextrose broth at 25°C for 48 hs, while, bacteria strains were cultured in Müller-Hinton broth.

At 37°C for 20 h before the test. 100 µL of standardized suspensions for each culture, according to Mc-Farland scale (1.3 × 10⁶ CFU/mL) of fungi were placed on Sabouraud Dextrose plate and the same cell count of bacteria were placed on Müller-Hinton agar plates using sterile cotton swab Discs of sterilized filter paper (6 mm) were loaded with tested compound and subjected to the inhibition zone tests. The discs

were aseptically placed on *Aspergillus flavus*, *Candida albicans*, *Aspergillus terreus*, *Staphylococcus aureus*, *Bacillus subtilis*, *Bacillus cereus*, *Escherichia coli*, *P vulgaris* culture plates. The agar plates of fungi were incubated for 48 h at 25°C, on the other hand, agar plates of bacteria were incubated for 24 hours at 37°C. The relative antimicrobial effect was obtained by measuring the clear zones of inhibition formed around the discs using a Vernier caliper instrument. Sabouraud Dextrose broth, Sabouraud Dextrose agar, Müller-Hinton broth, and Müller-Hinton agar media were prepared by dis. water. The antimicrobial test for all microorganisms was made in triplicate.¹⁶

Biochemical Studies

This study was designed to involve a series of *in vitro* and *in vivo* investigations as follows.

In vitro study. EA-GaNPs cytotoxicity on MCF-7 cell line cytotoxicity of EA-GaNPs was evaluated on the human breast cancer (MCF-7) cell line using the 3-(4, 5-dimethylthiazol-2-yl)-2, 5-diphenyltetrazolium bromide (MTT) assay¹⁷ which based on the mitochondrial dehydrogenase conversion of the MTT to a blue formazan product in the viable cells by an enzyme present in the mitochondria of viable cells. The colorimetric changes of blue formazan dissolved in dimethyl sulfoxide (DMSO) were measured spectrophotometrically at 570 nm using an enzyme-linked immunosorbent assay (ELISA) plate reader DV990BV4 microplate reader from Gio. de Vita E C. S.r.l (Rome, Italy) and data were analyzed using 990-win 6 software.

In vivo study

EA-GaNPs LD50. The median lethal dose which caused death to 50% of the population of the experimental animals was determined according to Bass¹⁸ by administration of ascending doses of the EA-GaNPs ranging from 1.5 to 50 mg/kg b.w. with an increasing factor (2.0) by oral gastric intubation to female Swiss albino rats (weighing about 120 ± 20 gm), mortality was recorded after 24 hours and LD 50 was calculated as following:

Log LD50 = Log LD next below 50% + (Log increasing factor x proportionate distance).

Proportionate distance

$$\frac{50\% - \text{mortality next below } 50\%}{\% \text{ mortality above } 50\% - \text{mortality next below } 50\%} \quad (1)$$

Experimental Design. Sixty Female Swiss albino rats weighing (120 ± 20 gm) are equally divided randomly into the following 4 groups:

Group I: Rats Were Served as Normal control

Group II: Rats were received a single dose of DMBA (20 mg/kg b.w. dissolved in 1.0 mL of olive oil) by oral

gastric intubation according to Tabaczar¹⁹, then animals were left till the end of the experiment (8 months) for carcinogenesis induction and they were palpated weekly to monitor changes in the mammary glands.

Group III: Rats have received a daily oral dose of 1.0 mg of EA-GaNPs/kg b.w. (1/10 of LD50) at the seventh month, by gastric intubation for one month.

Group VI: Rats received a single dose of DMBA as in group II at the seventh-month rats received EA-GaNPs daily for one month as in group III.

Samples Collection:

At the end of the experiment (after 8 months), rats were fasted overnight then anesthetized using diethyl ether. Blood samples were obtained via heart puncture and collected in plain vacutainer tubes. Immediately after blood sampling, animals were sacrificed and Mammary glands were excised from animals in all groups. A portion of mammary glands was homogenized (10% w/v) in phosphate-buffered-saline (.02 M sodium phosphate buffer with .15 M sodium chloride, pH7.4) using glass homogenizer producing homogenates which were used for biochemical and molecular analysis. The other portion was quickly rinsed in 10% formalin for histopathological examination.

Biochemical Analysis. The activity of alanine transaminase (ALT) and aspartate aminotransferase (AST) were estimated by the procedure described by Reitman and Frank²⁰ using diagnostic kits purchased from Biodiagnostic Company, Egypt. Serum creatinine and urea were determined by procedures described by Bartels²¹ and Patton and Crouch,²² respectively, using diagnostic kits purchased from Diamond Company, Egypt. Superoxide dismutase (SOD) activity was determined according to the method of Minami and Yoshikawa²³ and reduced glutathione (GSH) was determined according to the method of Beutler.²⁴ Lipid peroxidation was evaluated by the determination of malondialdehyde (MDA) concentration according to the method of Yoshioka²⁵. Total iron-binding capacity (TIBC) and serum calcium were measured according to the methods described by Bauer²⁶ and Shin,²⁷ respectively, using diagnostic kits purchased from Spectrum Company, Egypt. Concentration of caspase-3 was determined using an ELISA kit from Biomatik Company (Biomatik, Ontario, Canada) which based on Sandwich-ELISA principle.

Western Blotting for Quantifying of Phosphatidyl Inositide 3-kinases and Protein Kinase B in Mammary Gland Tissue. Mammary gland content of PI3K and AKT was evaluated by western blot technique according to Towbin²⁸. Tissue protein was extracted using TRIzol reagent according to Wu,²⁹ then protein concentration was estimated according to Lowry³⁰ using the Thermo Scientific Modified Lowry Protein Assay kit, and β -actin antibody (Proteintech, USA) as a loading control.

Histopathological Findings. Mammary glands were fixed in 10% formalin, dehydrated using gradient alcohol concentrations

and embedded in paraffin wax. Sections of 5 mm thickness were cut off paraffin wax cubs and stained with hematoxylin and eosin 33 and examined by light microscope Banchroft.³¹

Gamma Irradiation Facility

Nanoparticle synthesis mixture was irradiated at a dose level of 50 kGy in the Gamma chamber 4000—A India, irradiation facility, at the National Center for Radiation Research and Technology (NCRRT), Atomic Energy Authority, Cairo, Egypt at a dose rate (1.170 kGy/h).

Statistical Analyses

Data analyses were performed using the SPSS (version 20). Data were analyzed with a one-way analysis of variance (ANOVA) followed by a post hoc test (LSD) for multiple comparisons. The results were expressed as mean \pm standard deviation (SD) for $n = 6$. Results were considered statistically significant at P values $\leq .05$.

Results

Characterization of EA-GaNPs

Dynamic Light Scattering (DLS). Sample of EA-GaNPs was analyzed by (DLS Zetasizer Nano ZS ZEN 3600, Malvern, UK) for size determination and the results revealed that EA-GaNPs size ranged from 5.8-10.5 nm, (Figure 1A).

Ultraviolet-visible Absorption (UV/VIS) Spectroscopy. UV/VIS spectroscopy absorbance of EA-GaNPs using the visible range revealed a major peak at 380 assigned to surface plasmon resonance of the nanoparticles and a narrow peak at 360 nm, (Figure 1B)

Transmission Electron Microscope Analysis. The physical morphology and size distribution of the EA-GaNPs was visualized by Scanning Microscope and the results revealed that EA-GaNPs were spherical with a relatively narrow particle size distribution range between 50.8 and 100.5 nm (Figure 1C).

Fourier Transforms Infrared (FT-IR) Spectroscopy. The FT-IR spectra of EA and EA-GaNPs samples are shown in Figure 2A and B, respectively. The spectrum of EA reveals strong broadband at 3286 cm^{-1} assigned to the O-H stretch, a weak band at 2116 cm^{-1} to the aromatic bending mode of C-H, a medium band at 1636 cm^{-1} to stretching vibration of C=C bond, and a peak at 585 cm^{-1} to C-H stretching vibration. Meanwhile, the FT-IR spectrum of EA-GaNPs exhibits the same vibrational bands as EA except for a new small peak that appeared around 952 cm^{-1} that is assigned to the Ga-OH deformation mode of a GaO(OH) moiety. This result can be taken as evidence of the interaction of Ga and EA, that the hydroxyl group of EA acts as a capping agent in controlling the GaNPs size.

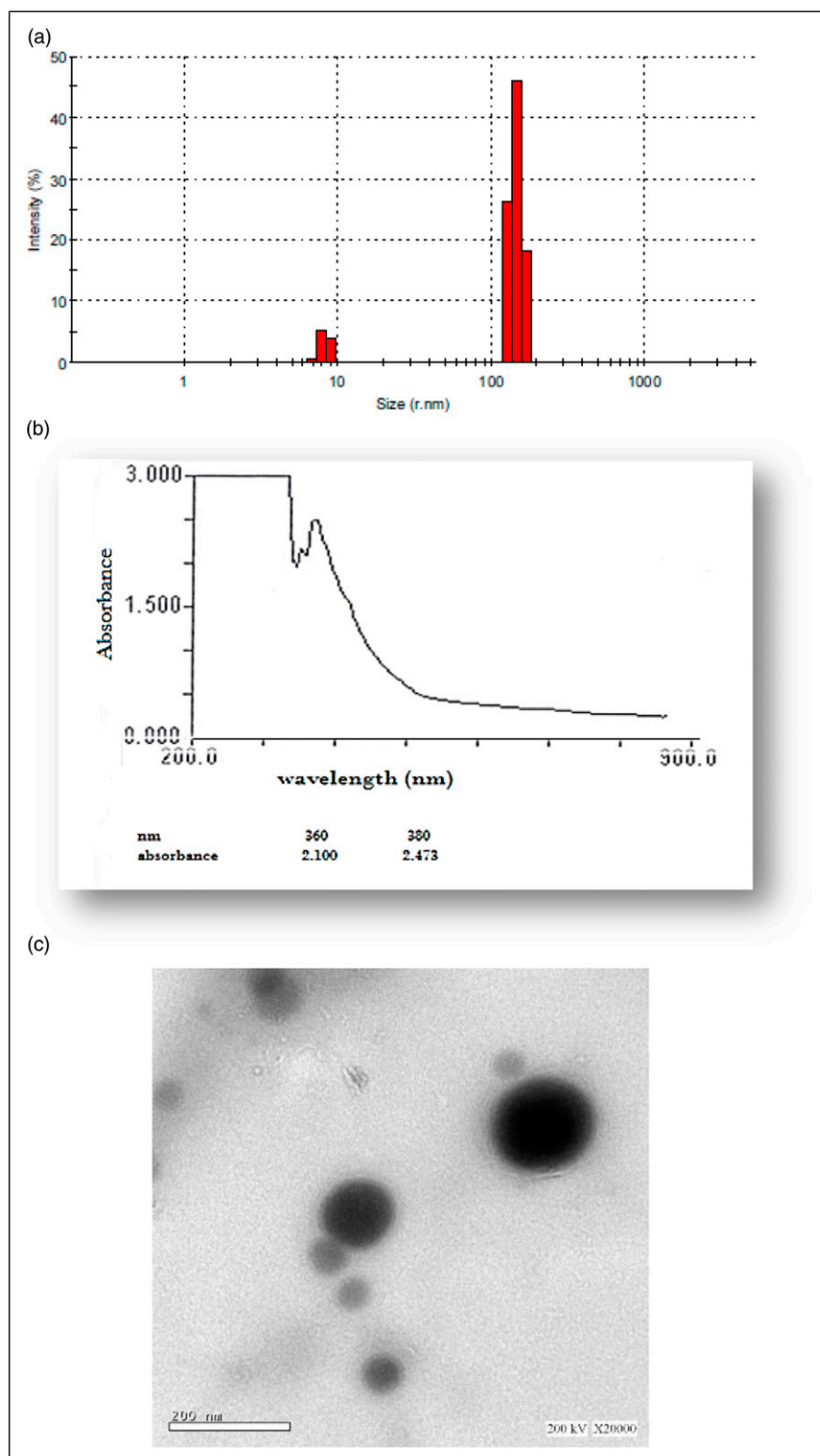


Figure 1. Characterization of synthesized EA-Ga NPs. (A) DLS analysis, (B) Ultraviolet-visible absorption (UV-VIS), (C) Transmission electron microscope with a magnification $\times 20,000$, bar =200 nm.

Antimicrobial Activity of EA-Ga NPs

Evaluating antimicrobial activity of EA-Ga NPs (1 mg/1 mL) revealed moderate toxicity behavior against Gram-positive (*Staphylococcus aureus*, *Bacillus subtilis*, *Bacillus cereus*) and Gram-negative pathogenic bacteria (*Escherichia coli*, *Proteus vulgaris*) also, antifungal activity was detected against (*Aspergillus terreus*), (Table.1).

EA-Ga NPs Toxicity Against MCF-7. EA-Ga NPs induce cytotoxicity effect on MCF-7 observed as a reduction in cell viability relative to the control in a dose-response manner. The EA-GaNPs concentration which reduced MCF-7 cell count to 50% (IC₅₀) is 2.86 ± .3 µg/ml (Figure 3)

In Vivo Study

The LD50 of EA-GaNPs. Ascending doses of the tested EA-GaNPs ranged from 1.5 to 50.0 mg/kg b.w. With increasing factor (2) were administered by oral gastric intubation to female Swiss albino rats (weighing about 120 + 20 gm), mortality was recorded after 24 hours. The median lethal dose (LD50) of EA-GaNPs was approximately 10.0 mg/kg b.w.

Effect of EA-GaNPs on Liver and Kidney Function Markers. DMBA administration resulted in significant elevation of serum levels of ALT, AST, urea, and creatinine compared with the normal healthy control which was reduced significantly by treating with EA-GaNPs and that was shown in (Table 2).

EA-GaNPs Effect on Oxidative Stress and Antioxidant Parameters. The oxidative stress and antioxidant status in the mammary tissues of the DMBA group were disrupted which was noticeable by a significant increase in MDA content and significant decrease of SOD activity and GSH content compared to normal control, the condition which was modified by treating with EA-GaNPs as MDA content was significantly decreased and SOD activity and GSH content were significantly increased (Table 3).

Effect of EA-GaNPs on serum values of TIBC, calcium, and caspase-3. DMBA administration significantly decreased Ca concentration and increased TIBC values compared to healthy control in serum which was reversed by treating with EA-GaNPs. Also, DMBA slightly increase the concentration of caspase-3 and increased AKT & PI3K protein intensity in mammary tissue. Meanwhile, the administration of EA-GaNPs decreased AKT & PI3K protein intensity, while the concentration of caspase-3 was significantly elevated (Figures 4 and 5).

Histopathological Studies. Histopathological examination of mammary gland tissues of DMBA group under light microscope showed alterations in the architecture of the glands as the lining epithelial cells of the acini and lactiferous ducts showed proliferative hyperplasia with cystic dilatation as well

as stratification. Treatment of DMBA-induced rats with EA-GaNPs showed a mild recurrence of normal mammary tissue appearance with mild stratification of the acinar lining epithelium (Figure 6)

Discussion

The current study was designed aiming to evaluate the anti-tumor efficacy of gallium nanoparticles coated by ellagic acid (EA-GaNPs) in *in vitro* on the viability of the human breast cancer cell line (MCF-7) and in *in vivo* against 7, 12 dimethyl benz[a] anthracene (DMBA)—induced mammary gland carcinogenesis in female Swiss albino rats, as well as its antimicrobial activity, was evaluated in comparison with standard antibiotics.

The biosynthesized EA- GaNPs were characterized via DLS and TEM for size dimension determination and visualization of the physical morphology and size distribution which revealed that EA-GaNPs were of spherical shape with relatively narrow particle size distribution ranged from 50.8–100.5 nm indicating their low scale as the size of nanoparticles is an important factor which significantly influences their biological activity.³² In addition, ultraviolet-visible (UV/VIS) absorbance spectroscopy showed two narrow peaks at 360 and 380 nm and this result is in agreement with others³³ who found that gallium is sensitive to ultraviolet radiation below 365 nm wavelengths. Also, these results are in line with a previous study³⁴ who reported that the UV/VIS spectrum for GaNPs showed a peak at 265 nm. Furthermore, the FT-IR spectra of the EA and EA-GaNPs were investigated as FT-IR enables the in-situ analysis of interfaces to investigate the surface adsorption of functional groups on nanoparticles³⁵ and it can be used to identify the possible biomolecules responsible for capping and efficient stabilization of the synthesized metal NPs, The spectrum of EA reveals strong broadband at 3286 cm⁻¹ assigned to the O-H stretch, a weak band at 2116 cm⁻¹ to the aromatic bending mode of C-H, a medium band at 1636 cm⁻¹ to stretching vibration of C=C bond, and a peak at 585 cm⁻¹ to C-H stretching vibration. Meanwhile, the FT-IR spectrum of EA-GaNPs exhibits the same vibrational bands as EA except for a new small peak that appeared around 952 cm⁻¹ that is assigned to the Ga-OH deformation mode of a GaO(OH) moiety as reported with others.³⁶ This result can be taken as evidence of the interaction of Ga and EA, that the hydroxyl group of EA acts as a capping agent in controlling the GaNPs size.

The emerging infectious diseases and the development of multi-drug resistance in the pathogenic bacteria and fungi at an alarming rate is a matter of serious concern. Evaluating antimicrobial activity of EA-Ga NPs (1 mg/1 mL) revealed moderate toxicity behavior against Gram-positive (*Staphylococcus aureus*, *Bacillus subtilis*, *Bacillus cereus*) and Gram-negative pathogenic bacteria (*Escherichia coli*, *Proteus vulgaris*) also, antifungal activity was detected against (*Aspergillus terreus*). The NPs are potential broad-spectrum antibiotics because they can inhibit a wide range of multidrug-resistant

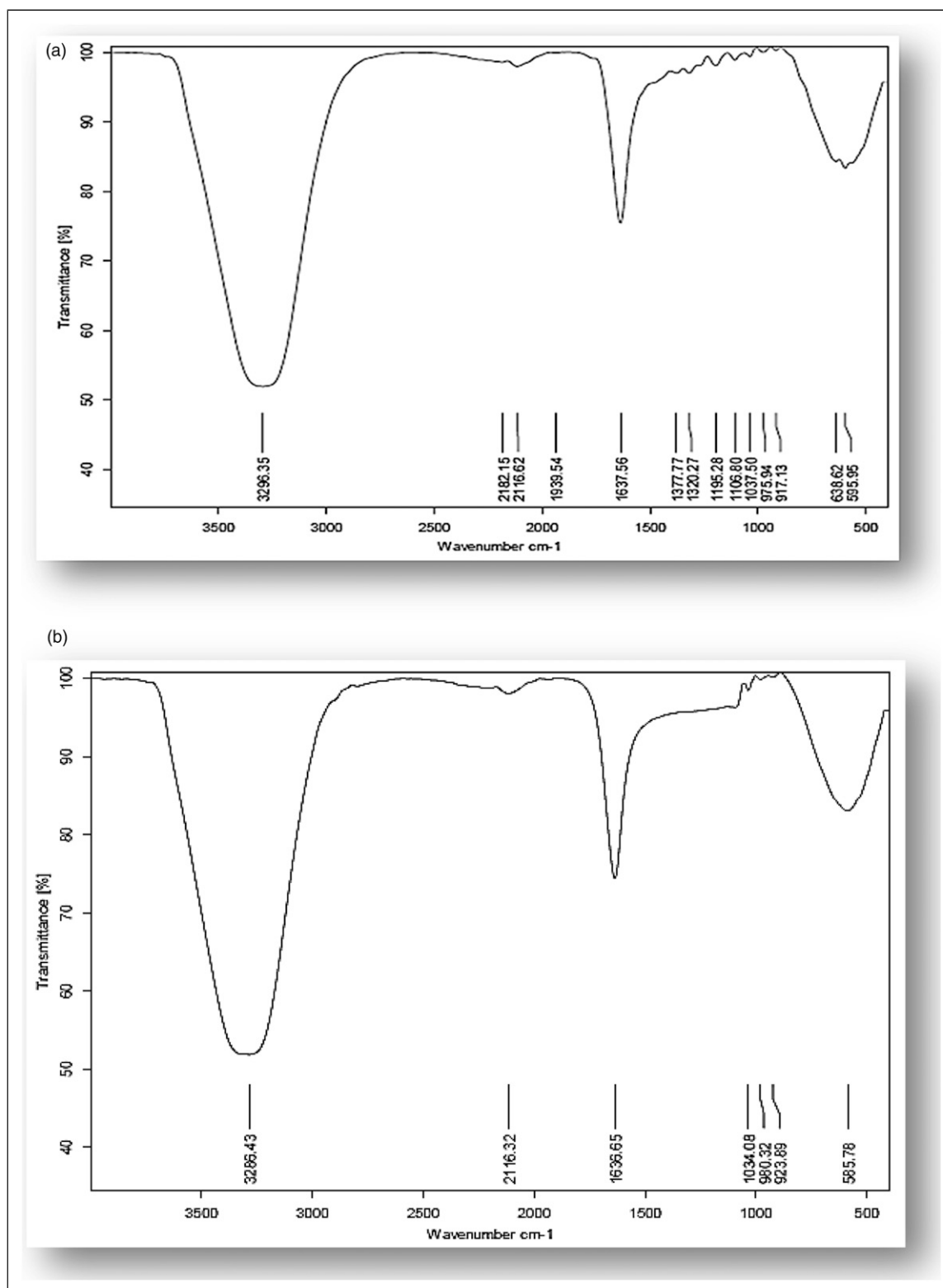


Figure 2. FT-IR spectrum of (A) Ellagic acid, (B) EA-GaNP.

Table 1. Antimicrobial Activity of EA-Ga NPs.

Fungi	Inhibition Zone (mm)	Reference Drug Ketoconazole (100 Qg/mL)
<i>Aspergillus flavus</i>	NA	16 ± 1.7
<i>Candida albicans</i>	NA	20 ± 2.1
<i>Aspergillus terreus</i>	1.2 ± 0.2	17 ± 1.9
Gram positive bacteria		Gentamycin (4 pg/mL)
<i>Staphylococcus aureus</i>	14 ± 1.2	24 ± 2.3
<i>Bacillus subtilis</i>	11 ± 1.1	26 ± 2.9
<i>Bacillus cereus</i>	1.2 ± .07	21 ± 2.3
Gram negative bacteria		Gentamycin (4 pg/mL)
<i>Escherichia coli</i>	12 ± 1.5	30 ± 2.7
<i>Proteus vulgaris</i>	10 ± 0.9	25 ± 2.1

Table 2. Effect of EA-GaNPs on Serum Levels of ALT, AST, Urea and Creatinine.

Groups	ALT (U/L)	AST (U/L)	Urea (mg/dl)	Creatinine (mg/dl)
Control	16.7 ± 4.04 ^b	12.2 ± 1.9 ^b	41 ± 8.7 ^b	.14 ± .03 ^b
DMBA	47.5 ± 5.5 ^a	36.3 ± 4.04 ^a	81.3 ± 8.5 ^a	.89 ± .11 ^a
EA-GaNPs	18.7 ± 3.05 ^b	16.0 ± 1.7 ^b	39.3 ± 9.5 ^b	.25 ± .04 ^b
DMBA+EA-GaNPs	31.7 ± 4.5 ^{a,b}	26.7 ± 2.5 ^{a,b}	57.3 ± 4.04 ^{a,b}	.49 ± .04 ^{a,b}

Data are expressed as Mean ± Standard Deviation.

^aSignificance versus control group.

^bSignificance versus DMBA group.

Table 3. EA-GaNPs Effect on MDA Level, SOD Activity and GSH Content in the Mammary Tissue.

Groups	MDA (nmol/mg protein)	SOD (U/mg protein)	GSH (mg/mg protein)
Control	10.9 ± .99 ^b	4.23 ± .76 ^b	69.8 ± 9.98 ^b
DMBA	42.9 ± 4.40 ^a	1.03 ± .17 ^a	30.3 ± 2.70 ^a
EA-GaNPs	9.6 ± 1.420 ^b	3.90 ± .74 ^b	72.7 ± 2.96 ^b
DMBA+EA GaNPs	22.5 ± 2.90 ^{a,b}	2.60 ± .21 ^{a,b}	51.8 ± 7.80 ^{a,b}

Data are expressed as Mean ± Standard Deviation.

^aSignificance versus control group.

^bSignificance versus DBMA group.

strains of bacteria that have defied most antibiotic treatment. Nanoparticles are nano-sized molecules (usually less than 100 nm in diameter) with a large surface area to volume ratio, which helps them to easily penetrate bacterial cells. The electrostatic interaction of nanoparticles with negatively-charged bacterial surfaces draw the particles to the bacteria and promotes their penetration into the membrane. The potential of a nanoparticle promotes nanoparticle interactions with cell membranes leading to membrane disruption, bacterial flocculation, and a reduction in viability. The generation of reactive oxygen species is also a mechanism of nanoparticle antibacterial activity.³⁷

Further mechanisms of action of nanoparticles as antimicrobial agents include disrupting deoxyribonucleic acid during the replication and cell division of microorganisms, compromising the bacterial membrane integrity via physical interactions with the microbial cell (the physical presence of a

nanoparticle most likely disrupts cell membranes in a dose-dependent manner), and releasing toxic metal ions and possessing abrasive properties which bring about lysis of cells.

Regarding the *in vitro* toxicity of EA-GaNPs against MCF-7, the result revealed a significant reduction of cell viability relative to control in a dose-response manner and that was in agreement with several studies in which the activity of gallium compounds has been observed in several cancer cell lines, including those for leukemia,³⁸ breast cancer,³⁹ hepatocellular carcinoma⁴⁰ and lymphoma.⁴¹ It was found that Ga modifies the three-dimensional structure of DNA and inhibits its synthesis and modulates protein synthesis. Also, it inhibits the activity of several enzymes, such as ATPases, DNA polymerases, ribonucleotide reductase, and tyrosine-specific protein phosphatase. Ga alters plasma membrane permeability and mitochondrial functions.¹⁰ Also, EA was found to induce apoptosis in cancer cells.⁴² However, the median Lethal Dose

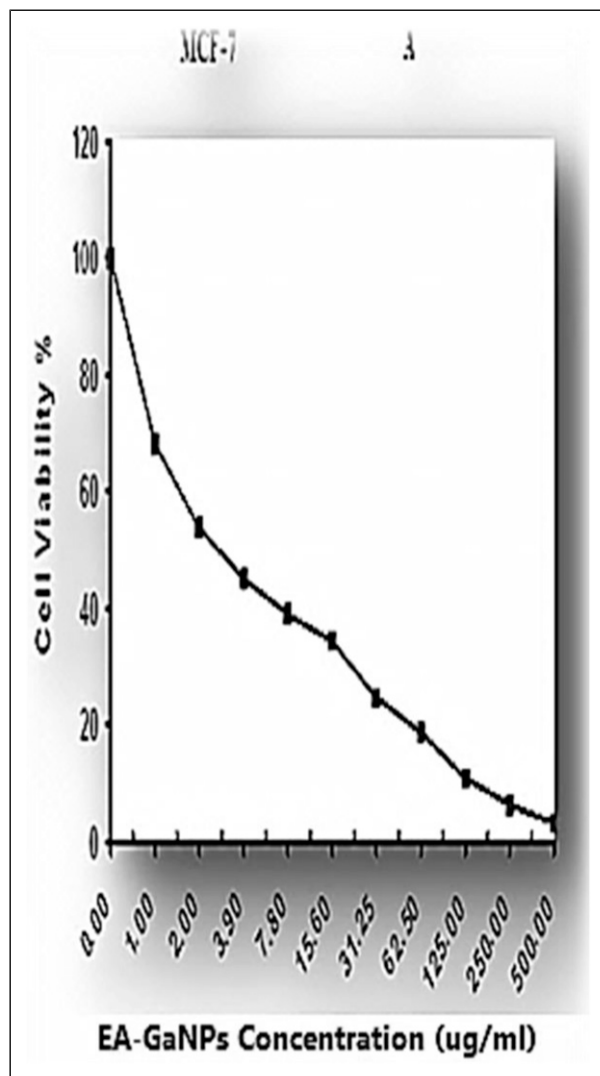


Figure 3. Antitumor efficacy of EA-GaNP against human breast cancer cell line (MCF-7).

(LD50) of EA–GaNP did not show any signs of toxicity in normal, healthy female rats.

It was found that DMBA damages many internal organs including the liver, by inducing the production of ROS, DNA adduct formation and affecting the activities of phase I, II, antioxidant and serum enzymes⁴³ and consequently the activities of ALT and AST were found to be significantly increased in all DMBA–treated groups compared to control groups of several studies^{43–46} that have been conducted as that are in line with the current study in which a significant elevation in the activities of ALT & AST in the serum of DMBA treated group was noted compared to the control group. Meanwhile, the administration of EA-GaNP to the DMBA-treated group improved the elevation in the activities of ALT & AST compared with the DMBA group and that was agreed with others.^{47,48}

DMBA administration also resulted in a significant increase in serum levels of urea and creatinine compared to the

control group which was in harmony with previous studies^{44,45} which indicate damage in kidneys due to DMBA induced toxicity, the effect that was reversed by administration of EA-GaNP as the results showed a significant decrease of serum urea and creatinine levels compared to the DMBA group which was in line with a previous study⁴⁷ in which tumor-induced rat groups treated with their novel compound, Betaine Tetrachloro-Gallate (BTG) complex have displayed significant decreases of plasma urea and creatinine levels with respect to DMBA-treated rats.

Administration of DMBA requires metabolic activation which produces radical cations, free radicals, and oxygenated metabolites,⁴⁹ and that was manifested in the current study through the significant increase of the MDA (lipid peroxidation marker) content within the mammary tissue homogenates by DMBA administration compared to the normal control group which was in agreement with others,^{50,51} this increase is attributed to the induction of DMBA to high levels of oxidative stress which resulted in the peroxidation of cell membrane lipids by generating of lipid peroxides.^{50,52} On the other hand, treatment with EA-GaNP in DMBA-treated rats resulted in a significant reduction of MDA content with respect to the DMBA group. The significant reduction in lipid peroxidation level by EA-GaNP may be attributed to the effect of EA which has been shown to exert a potent scavenging action on superoxide anion and hydroxyl anion *in vitro*, as well as the protective effect against lipid peroxidation.⁵³

Additionally, DMBA-treated rats significantly decreased the activity of SOD activity and GSH content compared with the normal group which may be due to their utilization during scavenging of the free radicals produced by DMBA.^{49,54} While treating of DMBA-group with EA-GaNP significantly increased SOD activity and GSH content compared to DMBA-group which may be due to the effect of EA. As it was found that the primer mechanism of action of EA has been defined as being able to counter the negative effects of oxidative stress by aiding the regeneration of cellular antioxidants such as GSH and ascorbate and by the activation or the induction of genes responsible for expressing enzymes such as SOD, CAT, GST and NADPH: quinone oxidoreductase.⁵⁵ Also, that significant increase of SOD and GSH may be a response to elevated levels of (O₂•) as a result of ROS generated by gallium administration.⁵⁶

Based on gallium's action on iron homeostasis due to its irreducible mimic action with Fe⁺³ which affects several cellular functions,⁵⁷ alterations of Fe-binding capacity (TIBC) values were studied whereas the DMBA-treated group showed a significant elevation in the value of TIBC regarding the normal group which attributed to a greater requirement of malignant cells for iron which may result in decreasing of serum iron concentration as shown in previous results of others⁵⁸ when 43% of the studied cases with breast cancer had depressed serum iron levels, where the mean serum iron levels in rats with breast cancer were significantly lower than those in the control group. So it has been suggested that the

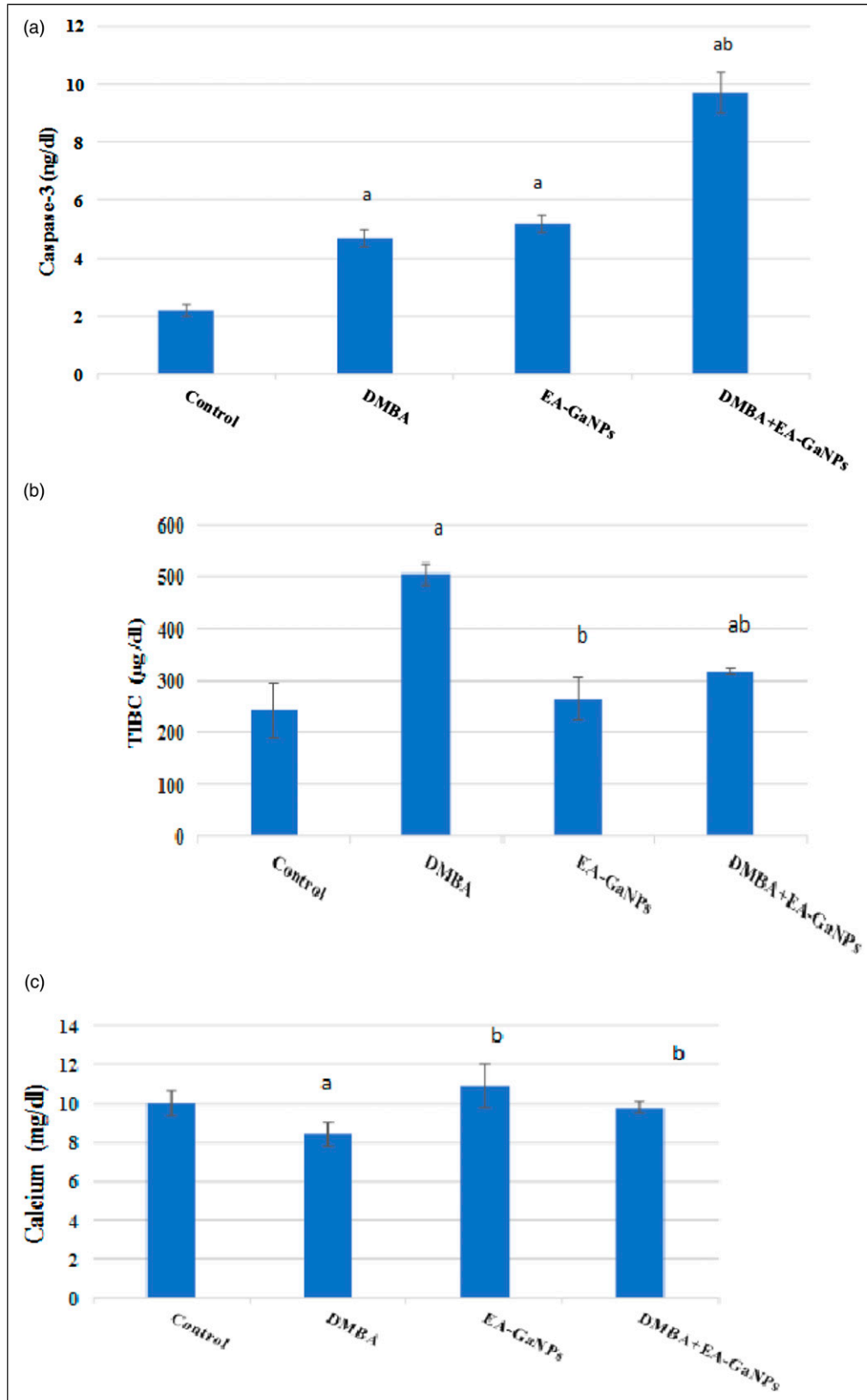


Figure 4. EA-Ga NPs effect on (A) mammary tissue caspase-3 concentration, (B) serum TIBC level and (C): serum calcium level. ^a significance vs the control group. ^b significance versus DMBA group.

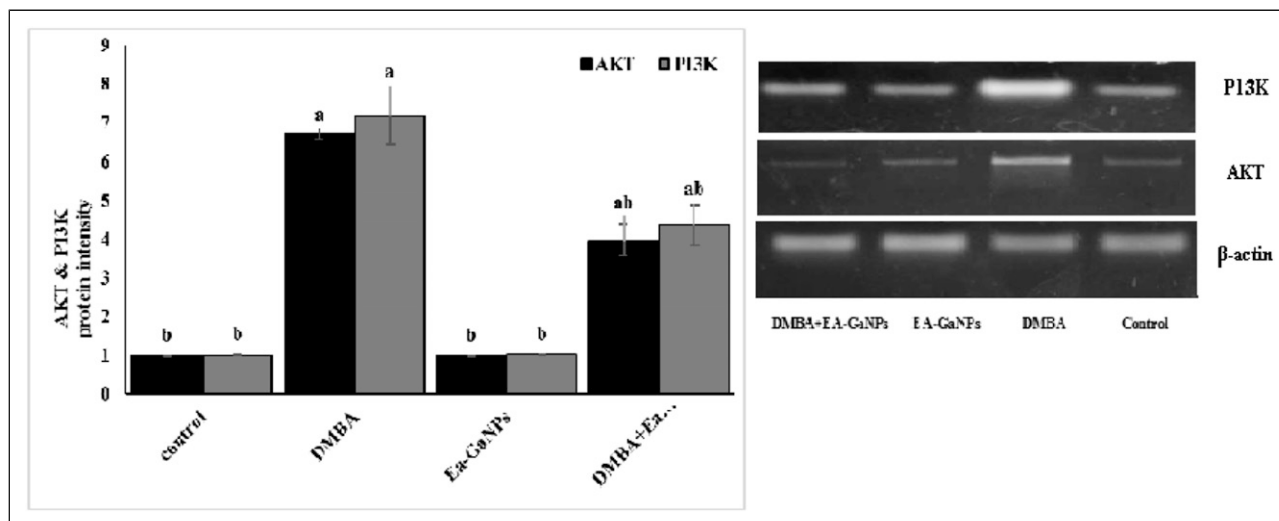


Figure 5. Western immunoblotting analysis of AKT & PI3K protein intensity in the mammary tissue.

neoplastic process in the organism significantly decreases iron concentration in the serum as it probably directs the iron to the developing tumor.⁵⁹ And without any doubt, the reduction of serum iron concentration results in increasing in TIBC values which were obviously in results of others,⁴⁷ the study revealed that DMBA-treated rats have a merely significant increase in TIBC mean concentration with respect to normal control rats.

On the other hand, DMBA-induced rats treated with EA-Ga-NPs showed a significant decrease in TIBC value compared to the DMBA group. Ga can bind to both metal binding sites on transferrin and under physiologic conditions, only about one-third of circulating transferrin is occupied by Fe, leaving the remaining two-thirds free to bind and transport gallium as transferrin-gallium complexes,⁴¹ which consequently results in decreasing of TIBC concentration. Our result was in harmony with a previous study⁴⁷ in which the administration of their novel compound (BTG) complex to tumor-bearing rats was found to significantly reduce plasma Fe and TIBC compared to the DMBA group.

It was found that calcium plays a dual role by its involvement in both proliferation/activation and apoptosis of both cancer and immune cells.⁶⁰ So it was an important issue to track the alterations of the calcium concentration in our study.

The present study showed that DMBA administration decreased the concentration of serum calcium which may be due to the immunosuppressive effect of DMBA as it was found in several studies that DMBA affect the activation and apoptosis of B and T-cells and natural killer (NK) cells by inhibiting of Ca^{2+} mobilization inhibiting of Ca^{2+} mobilization or altering effect on Ca^{2+} homeostasis which was correlated with an increase in baseline levels of cytoplasmic free Ca^{2+} (intracellular Ca^{2+}).^{61,62} That inhibition of Ca^{2+} mobilization and increasing of intracellular Ca^{2+} may be the reason for the decreasing of serum calcium level which may mean the importing of Ca^{2+} into the cytosol to affect the immune cells as transient small

elevations (low to medium nM) of cytosolic Ca^{2+} will increase cell proliferation whereas sustained substantial elevations (high nM to μ M) may induce apoptosis.⁶³

On the other hand, the current results showed that the administration of EA-Ga-NPs to DMBA-treated rats showed a significant increase in the concentration of serum calcium which reversed the decrease induced by DMBA. For as much the vital role of Ca^{2+} in the physiology and biochemistry of organisms and the cell and its regulation by various parameters, several researches are needed to study its involvement in each pathological condition.

Considering the central role of caspase-3 in executing apoptosis and the several observations that established breast cancer cell lines exhibit altered caspases-3 expression⁶⁴. Cagnol⁶⁵ reported that caspase-3 and 9 levels were significantly decreased in several cancers. Considering the central role caspase-3 plays in executing apoptosis, it has been suggested that the loss of caspase-3 expression represents a selective event or lesion in breast cancer cells.⁶⁴ Furthermore, upon determining the levels of caspase-3 in a panel of human mammary cancer cell lines⁶⁶ observed that several breast cancer cell lines; MCF-7, BT-20T and ZR-75T, exhibit a complete lack of caspase-3 protein expression. On contrary, the current study showed that challenging female albino rats with DMBA resulted in a slight increase of caspase-3 concentration compared to the normal control, however, this increase is still below the level of significance. This finding would appear to conflict with the widely held belief that apoptosis is reduced in malignancy. The proliferation/apoptosis ratio, however, may be higher in DMBA-treated mammary glands than in the corresponding normal glands,⁶⁷ hence this increase in caspase-3 concentration was non-significant.

On the other hand, a noted increase in the concentration of caspase-3 was observed upon the administration of EA-Ga-NPs to DMBA-treated rats compared to DMBA-treated group and

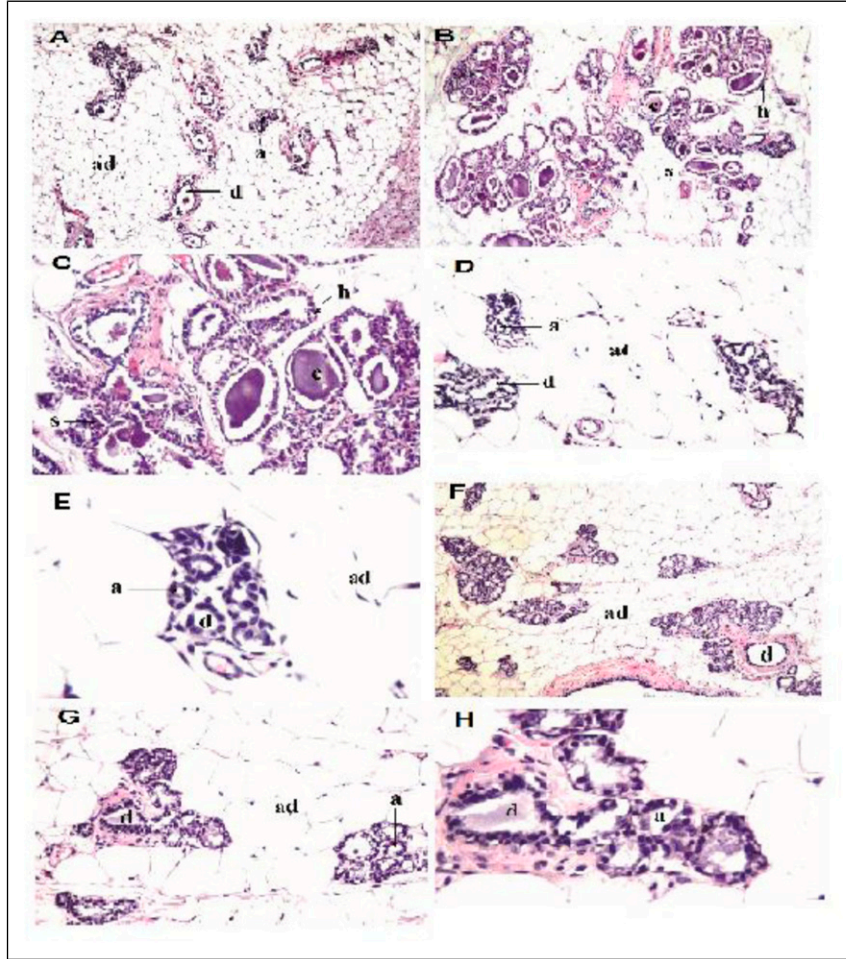


Figure 6. Photomicrograph of mammary gland sections in different experimental rat groups. (A) Control group; normal histological structure of the acini (a) and ducts (d) embedded in adipose tissue (ad), (H&E, 16X), (B) DMBA group; histopathological alterations in the architecture of the glands as the lining epithelial cells of the acini and lactiferous ducts showed proliferative hyperplasia (h) with cystic dilatation (c) as well as stratification (s), (H&E, $\times 16$), (C) DMBA group; magnification of the cystic ductal dilatation(c) and the stratification (s) of the lining epithelium of the acini, (H&E, 40X). (D) EA-GaNPs group; normal histological structure of the acini (a) and ducts (d) embedded in adipose tissue, (H&E, 40X). (E) EAGaNPs group; magnification of the normal histological structure of the acini (a) and ducts (d) embedded in adipose tissue, (H&E, 80X), (F) DMBA+EA-GaNPs group; mild recurrence of normal mammary tissue histological structure with mild stratification of the acinar lining epithelium, (H&E, $\times 16$), (G) DMBA+EA-GaNPs group; magnification of the mild stratification of the acinar lining epithelium, (H&E, $\times 40$) and (H) DMBA+EA-GaNPs group; magnification of the mild stratification of the acinar lining epithelium, (H&E, 80X).

that agreed with others.⁴⁷ This result attributed to one of the known apoptotic mechanisms of Ga which are associated with activation of caspase-3 as it was found that the exposing of human leukemia/lymphoma cells to gallium nitrate or gallium maltolate resulted in initial translocation of inositol phosphatidylserine (an early marker of apoptosis) to the cell surface which followed by a loss of mitochondrial membrane potential leading to the release of cytochrome-C from the mitochondria to the cytoplasm and the activation of caspase-3 and morphological changes of apoptosis.⁶⁸ Also, the activation of the proapoptotic factor BAX and caspase-3 can be considered as a possible mechanism of cell death induced by Ga.⁶⁹

Due to the fact of relying on the basic mechanism of cancer development primarily on DNA damage-induced through

several protein clusters and pathways (signaling pathways). Currently, the DMBA-group displayed a significant increase of both of AKT & PI3K protein intensity/ β -actin protein expression in the mammary tissue homogenates compared to the normal control group indicating the stuck of PI3K/Akt signaling pathway in “on” position which resulting in cellular surviving and that agreed with a previous study⁷⁰ who performed whole-exome and RNA sequencing on long latency mammary tumors induced by DMBA and transcriptome profiling indicated a significant activation of the PI3K/Akt signaling pathway.

On the other hand, the treating of DMBA-group with EA-GaNPs revealed a significant decrease of both of AKT & PI3K protein intensity indicating that EA-GaNPs exert antitumor

potential via downregulation of that signaling pathway which may be due to the effect of EA which was found to induce apoptosis through reducing of the PI3K/AKT pathway.^{71,72} And those findings may be due to the effect of EA that decreases cell proliferation through a reduction of phosphorylated *STAT3*, ERK, and AKT cellular signaling proteins in human prostate cancer cells (PC3) as the Western blot data indicated a decrease in the cellular concentrations of pSTAT3, pAKT, and pERK1/2 signaling pathways in a dose-dependent manner of EA.

Histopathological sections of the mammary gland tissues of the DMBA-treated group showed histopathological alterations in the architecture of the glands with respect to the control group as the lining epithelial cells of the acini and lactiferous ducts showed proliferative hyperplasia with cystic dilatation as well as stratification. This result was agreed with a previous study⁷³ in which one of the observed histopathological alterations in a Sprague–Dawley (SD) rat model induced (DMBA) and estrogen–progesterone (E-P) was ductal epithelial hyperplasia. While the treating of DMBA-induced rats with EA-GaNP revealed a mild recurrence of normal mammary tissue appearance as there was no hyperplasia of the lining epithelium of the duct system and cystic ductal dilatation, the alterations that are observed in mammary tissue of DMBA-treated group, but there was a mild stratification of the acinar lining epithelium.

Acknowledgments

We wish to acknowledge the contribution of Dr Adel Bakeer, Professor of Pathology, Faculty of Veterinary Medicine, Cairo University, for assistance in setting up the histopathological study.

Declaration of Conflicting Interests

The author(s) declared no potential conflicts of interest with respect to the research, authorship, and/or publication of this article.

Funding

The author(s) received no financial support for the research, authorship, and/or publication of this article.

ORCID iDs

Fatma SM Moawad  <https://orcid.org/0000-0002-5792-0815>

Eman I Kandil  <https://orcid.org/0000-0003-4731-7315>

Supplemental Material

Supplemental material for this article is available online.

1. Bray F, Ferlay J, Soerjomataram I, Siegel RL, Torre LA, Jemal A. Global cancer statistics 2018: GLOBOCAN estimates of incidence and mortality worldwide for 36 cancers in 185 countries. *CA: A Cancer Journal for Clinicians*. 2018;68:394-424.
2. Bishayee A, Mandal A, Thoppil RJ, Darvesh AS, Bhatia D. Chemopreventive effect of a novel oleanane triterpenoid in a

- chemically induced rodent model of breast cancer. *Int J Cancer*. 2013;133(5):1054-1063.
3. Skandarajah AR, Bruce Mann G. Selective use of whole breast radiotherapy after breast conserving surgery for invasive breast cancer and DCIS. *Surgeon*. 2013;11(5):278-285.
4. Haq AI, Zabkiewicz C, Grange P, Arya M. Impact of nanotechnology in breast cancer. *Expert Rev Anticancer Ther*. 2009;9(8):1021-1024.
5. Soo V, Kwan B, Quezada H, et al. Repurposing of anticancer drugs for the treatment of bacterial infections. *Curr Top Med Chem*. 2017;17(10):1157-1176.
6. Singh OP, Nehru RM. Nanotechnology and cancer treatment. *Asian J. Exp. Biol. Sci*. 2008;22(2):6.
7. Seleci M, Seleci DA, Bongartz R, et al. Smart multifunctional nanoparticles in nanomedicine. *BioNanoMaterials*. 2016;17(1-2):33W1.
8. Nie S, Xing Y, Kim GJ, Simons JW. Nanotechnology Applications in Cancer. *Annu Rev Biomed Eng*. 2007;9(1):257-288.
9. Hasan S. A review on nanoparticles: their synthesis and types. *Res J Recent Sci*. 2015;4(ISC-2014):9-11.
10. Coltery P, Keppler B, Desoize CB. Gallium in cancer treatment. *Crit Rev Oncol Hematol*. 2002;42:283-296.
11. Chitambar CR. The therapeutic potential of iron-targeting gallium compounds in human disease: From basic research to clinical application. *Pharmacol Res*. 2017;115:56-64.
12. Zhang HM, Zhao L, Li H, Xu H, Chen WW, Tao L. Research progress on the anticarcinogenic actions and mechanisms of ellagic acid. *Cancer biology & medicine*. 2014;11(2):92-100.
13. Hussein RH, Khalifa FK. The protective role of ellagitannins flavonoids pretreatment against N-nitrosodiethylamine induced-hepatocellular carcinoma. *Saudi J Biol Sci*. 2014;21:589-596.
14. Janku F, Yap TA, Meric-Bernstam F. Targeting the PI3K pathway in cancer: are we making headway? *Nat Rev Clin Oncol*. 2018;15(5):273-291.
15. Li D, Liu Z, Yuan Y, et al. Green synthesis of gallic acid-coated silver nanoparticles with high antimicrobial activity and low cytotoxicity to normal cells. *Process Biochem*. 2015;50:357-366.
16. Pazos-Ortiz E, Roque-Ruiz JH, Hinojos-Marquez EA, et al. Dose-Dependent Antimicrobial Activity of Silver Nanoparticles on Polycaprolactone Fibers against Gram-Positive and Gram-Negative Bacteria. *J Nanomater*. 2017;2017. Article ID 4752314, 9 pages.
17. Wilson J, Sargent J, Elgie A, Hill J, Taylor C. A feasibility study of the MTT assay for chemosensitivity testing in ovarian malignancy. *Br J Cancer*. 1990;62:189-194.
18. Bass KF, Gunzel P, Henchler D. LD50 versus acute toxicity. *Arch Toxicol*. 1982;51:183-186.
19. Tabaczar S, Domeradzka K, Czepas J, et al. Anti-tumor potential of nitroxyl derivative Pirolin in the DMBA-induced rat mammary carcinoma model: A comparison with quercetin. *Pharmacol Rep*. 2015;67:527-534.
20. Reitman S, Frankel S. A Colorimetric Method for the Determination of Serum Glutamic Oxalacetic and Glutamic Pyruvic Transaminases. *Am J Clin Pathol*. 1957;28(1):56-63.

21. Bartels H, Böhmer M, Heierli C. Serum kreatininbestimmung ohne enteiuweisen. *Clin Chim Acta*. 1972;37:193-197.
22. Patton CJ, Crouch SR. Spectrophotometric and kinetics investigation of the Berthelot reaction for the determination of ammonia. *Anal Chem*. 1977;49:464-469.
23. Minami M, Yoshikawa H. A simplified assay method of superoxide dismutase activity for clinical use. *Clinica chimica acta; international journal of clinical chemistry*. 1979;92:337-342.
24. Beutler E, Duron O, Kelly BM. Improved method for the determination of blood glutathione. *J Lab Clin Med*. 1963;61:882-888.
25. Yoshioka T, Kawada K, Shimada T, Mori M. Lipid peroxidation in maternal and cord blood and protective mechanism against activated-oxygen toxicity in the blood. *Am J Obstet Gynecol*. 1979;135(3):372-376.
26. Bauer JD, Mosby Company. Haemoglobin, porphyrin, and iron metabolism. In: Kaplan LA, Pesce AJ, eds *Clinical Chemistry, Theory, Analysis, and Correlation*. 1984:611-655.
27. Shin DH, Yoon KJ, Kwon SK, et al. Determination of total calcium in serum with Arsenazo III method. *Korean J Clin Pathol*. 1994;14(1):12-19.
28. Towbin H, Staehelin T, Gordon J. Electrophoretic transfer of proteins from polyacrylamide gels to nitrocellulose sheets: procedure and some applications. *Proc Natl Acad Sci Unit States Am*. 1979;76:4350-4354.
29. Wu LC. Isolation and long-term storage of proteins from tissues and cells using TRIZOL reagent. *Focus*. 1997;17:98-100.
30. Lowry O, Rosebrough N, Farr AL, Randall R. Protein measurement with the Folin phenol reagent. *J Biol Chem*. 1951;193(1):265-275.
31. Bancroft JD, Stevens A, Turner DR. *Theory and Practice of Histological Techniques*. 4th edn. London, UK: Churchill Livingstone; 1996:125.
32. Shin S, Song I, Um S. Role of physicochemical properties in nanoparticle toxicity. *Nanomaterials*. 2015;5:1351-1365.
33. Eisenberg I, Alpern H, Gutkin V, Yochelis S, Paltiel Y. Dual mode UV/visible-IR gallium-nitride light detector. *Sensor Actuator Phys*. 2015;233:26-31.
34. Kandil EI, El-sonbaty SM, Moawed FS, Khedr OM. Anticancer redox activity of gallium nanoparticles accompanied with low dose of gamma radiation in female mice. *Tumour biology: The Journal of the International Society for Oncodevelopmental Biology and Medicine*. 2018;40(3):1010428317749676-14.
35. Mudunkotuwa IA, Minshid AA, Grassian VH. ATR-FTIR spectroscopy as a tool to probe surface adsorption on nanoparticles at the liquid-solid interface in environmentally and biologically relevant media. *The Analyst*. 2014;139:870-881.
36. Yang J, Zhao Y, Frost RL. Infrared and infrared emission spectroscopy of gallium oxide α -GaO(OH) nanostructures. *Spectrochim Acta Mol Biomol Spectrosc*. 2009;74:398-403.
37. Thekkae Padil VV, Černík M. Green synthesis of copper oxide nanoparticles using gum karaya as a biotemplate and their antibacterial application. *Int J Nanomed*. 2013;8:889-98.
38. Bernstein LR. Mechanisms of therapeutic activity for gallium. *Pharmacol Rev*. 1998;50:665-82.
39. Wang F, Jiang X, Yang DC, Elliott RL, Head JF. Doxorubicin-gallium-transferrin conjugate overcomes multidrug resistance: evidence for drug accumulation in the nucleus of drug resistant MCF-7/ADR cells. *Anticancer research*. 2000;20:799-808.
40. Chua MS, Bernstein LR, Li R, So SK. Gallium maltolate is a promising chemotherapeutic agent for the treatment of hepatocellular carcinoma. *Anticancer research*. 2006;26:1739-43.
41. Chitambar CR. Medical Applications and Toxicities of Gallium Compounds. *Int J Environ Res Publ Health*. 2010;7:2337-2361.
42. shirode AB, Bharali DJ, Nallanthighal S, Coon JK, Mousa SA, Reliene R. Nanoencapsulation of pomegranate bioactive compounds for breast cancer chemoprevention. *Int J Nanomed*. 2015;10:475-84.
43. Khyade VB. Influence of Sibinin on DMBA induced hepatotoxicity and free radical damage in Norwegian rat, *Rattus norvegicus*. *IJIRSET*. 2016;3(12):22-38.
44. Ozdemir I, Selamoglu Z, Ates B, Gok Y, Yilmaz I. Modulation of DMBA-induced biochemical changes by organoselenium compounds in blood of rats. *Indian Journal of Biochemistry & Biophysics*. 2007;44:257-9.
45. Bedi PS, Priyanka S. Effects of garlic against 7-12, Dimethyl benzanthracene induced toxicity in Wistar albino rats. *Asian J Pharm Clin Res*. 2012;5(4):170-173.
46. Arora R, Bhushan S, Kumar R, et al. Hepatic dysfunction induced by 7, 12-Dimethylbenz(o)anthracene and its obviation with Erucin using enzymatic and histological changes as indicators. *PLoS ONE* 2014;9(11):e112614.
47. Salem A, Noaman E, Kandil E, et al. Crystal structure and chemotherapeutic efficacy of the novel compound, gallium tetrachloride betaine, against breast cancer using nanotechnology. *Tumor Biol*. 2016; 37(8): 11025-1108.
48. Moustafa EM, Mohamed MA, Thabet NM. Gallium nanoparticle-mediated reduction of brain specific serine protease-4 in an experimental metastatic cancer model. *Asian Pac J Cancer Prev* 2017;18(4):895-903.
49. Batcioglu K, Uyumlu AB, Satilmis B, et al. Oxidative stress in the in vivo DMBA rat model of breast cancer: suppression by a voltage-gated sodium channel inhibitor (RS100642). *Basic Clin Pharmacol Toxicol* 2012;111:137-141.
50. Moselhy SS, Al mslmani MAB. Chemopreventive effect of lycopene alone or with melatonin against the genesis of oxidative stress and mammary tumors induced by 7, 12dimethyl (a) benzanthracene in Sprague dawely female rats. *Mol Cell Biochem*. 2008;319(1-2):175-180.
51. Hamdy SM, Latif AK, Drees EA, Soliman SM. Prevention of rat breast cancer by genistin and selenium. *Toxicol Ind Health* 2012 Sep;28(8):746-757. doi:10.1177/0748233711422732.
52. Selamoglu TZ, Yilmaz I, Ozdemir I, et al. Role of synthesized organoselenium compounds on protection of rat erythrocytes from DMBA- induced oxidative stress. *Biol Trace Elem Res* 2009;128:167-175.
53. Ozkaya A, Selik S, Yuce A, et al. The effects of ellagic acid on some biochemical parameters in the liver of rats against oxidative stress induced by aluminum. *KAFKAS UNIV VET. FAK* 2010;16(2):263-268.

54. Soujanya J, Silambujanaki P, Krishna VL. Anticancer efficacy of holoptelea integrifolia, planch. against 7,12-dimethylbenz(a) anthracene induced breast carcinoma in experimental rats. *Int J Pharm Pharm Sci* 2011;3:103-106.
55. Vattem DA, Shetty K. Biological functionality of ellagic acid: a review. *J Food Biochem* 2005(29):234-266.
56. Bériault R, Hamel R, Chenier D, et al. The over expression of NADPH- producing enzymes counters the oxidative stress evoked by gallium, an iron mimetic. *Biometals* 2007;20:165-176.
57. Chitambar CR. Gallium and its competing roles with iron in biological systems. *Biochim Biophys Acta* 2016;1863:2044-2053.
58. Elliott RL, Head JE, McCoy JL. Relationship of serum and tumor levels of iron and iron-binding proteins to lymphocyte immunity against tumor antigen in breast cancer patients. *Breast Cancer Res Treat* 1994;30:305-309.
59. Skrajnowska D, Bobrowska-Korczak B, Tokarz A, et al. Copper and resveratrol attenuates serum catalase, glutathione peroxidase, and element values in rats with DMBA-induced mammary carcinogenesis. *Biol Trace Elem Res* 2013;156(1-3):271-278.
60. Schwarz EC, Qu B, Hoth M. Calcium, cancer and killing: the role of calcium in killing cancer cells by cytotoxic T lymphocytes and natural killer cells. *Biochim Biophys Acta* 2013;1833(7):1603-1611.
61. Burchiel SW, Davis DA, Ray SD, Barton SL. DMBA induces programmed cell death (apoptosis) in the A20.1 murine B cell lymphoma. *Fundamental and applied TOXICOLOGY o cfa/ Journal Of the. Society of Toxicology* 1993;21(1):120-124.
62. Cao Y, Wang J, Henry-Tillman R, Klimberg VS. Effect of 7, 12-dimethylbenz[a]anthracene (DMBA) on gut glutathione metabolism. *J Surg Res* 2001;100(1):135-140.
63. Qu B, Al-Ansary D, Kummerow C, Hoth M, Schwarz EC. ORAI- mediated calcium influx in T cell proliferation, apoptosis and tolerance. *Cell Calcium* 2011;50:261-269.
64. Devarajan E, Sahin AA, Chen JS, et al. Down-regulation of caspase 3 in breast cancer: a possible mechanism for chemoresistance. *Oncogene* 2002(21):8843-8851.
65. Cagnol S, Mansour A, Van Obberghen-Schilling E, et al. Raf-1 activation prevents caspase 9 processing downstream of apoptosome formation. *J Signal Transduct* 2011;2011:1-12.
66. Jiinicke RU, Sprengart ML, Wati MR. et. al. Caspase-3 is required for DNA fragmentation and morphological changes associated with apoptosis. *J Biol Chem* 1998;273(16):9357-9360.
67. O'Donovan N, Crown J, Stunell H, et al. Caspase-3 in breast cancer. *Clin Cancer Res* 2003;9(2):738-742.
68. Chitambar CR. Gallium-containing anticancer compounds. *Future Med Chem* 2012;4(10):1257-1272.
69. Chitambar CR, Wereley JP, Matsuyama S. Gallium-induced cell death in lymphoma: role of transferrin Receptor cycling, involvement of Bax and the mitochondria, and effects of proteasome inhibition. *Mol Cancer Ther* 2006;5:2834-2843.
70. Abba MC, Zhong Y, Lee J, et al. DMBA induced mouse mammary tumors display high incidence of activating Pik3ca H1047 and loss of function Pten mutations. *Oncotarget* 2016; 7(39):64289-64299.
71. Wang N, Wang ZY, Mo SL, et al. Ellagic acid, a phenolic compound, exerts anti-angiogenesis effects via VEGFR-2 signaling pathway in breast cancer. *Breast Cancer Res Treat* 2012;134:943-955.
72. Eskandari E, Heidarian E, Amini SA, et al. Evaluating the effects of Ellagic acid on pSTAT3, pAKT, and pERK1/2 signaling pathways in prostate cancer PC3 cells. *J Cancer Res Ther* 2016; 12:1266-1271.
73. Feng M, Feng C, Yu Z, et al. Histopathological alterations during breast carcinogenesis in a rat model induced by 7,12-Dimethylbenz (a) anthracene and estrogen-progestogen combinations. *Int J Clin Exp Med* 2015;8(1):346-357.